A New Compressive Sensing Born Iterative Method to Image Non-Weak Scatterers

G. Oliveri, L. Poli, N. Anselmi, M. Salucci, and A. Massa

Abstract

In this work, the solution of the non-linear inverse scattering (*IS*) problem in presence of non-weak scatterers is dealt with. More in detail, a customized hybrid solution approach is developed based on the effective combination of the Born iterative method (*BIM*) formulation and a multi-task Bayesian compressive sensing (*MT-BCS*) solution approach. Thanks to the adopted strategy, it is possible to avoid the contrast source formulation (*CSF*) of the *IS* problem, as well as the use of time-consuming full-wave simulations for the computation of the electric field inside the imaged domain. Some numerical results are shown to verify the effectiveness of the proposed *IS* solution method when dealing with the imaging of different pixel-sparse targets under several noisy conditions.

Contents

1 Numerical Validation

1.1 E-shaped Object, $\ell_1 = \frac{5}{6}\lambda$, $\ell_2 = \lambda/2$

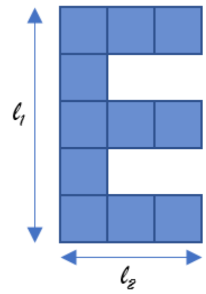

Figure 1: E-shaped Object

Test Case Description

Direct solver:

- Cubic domain divided in $\sqrt{D} \times \sqrt{D}$ cells
- Number of cells for the direct solver: $D = 1296$ (discretization $= \lambda/12$)

Inverse solver:

- Cubic domain divided in $\sqrt{N} \times \sqrt{N}$ cells
- Number of cells for the inversion: $N = 324$ (discretization $= \lambda/6$)

Measurement domain:

- Total number of measurements: $M = 27$
- Measurement points placed on circles of radius $\rho = 3\lambda$

Sources:

- Plane waves
- Number of views: $V = 4$; $\theta_{inc}^{v} = 0° + (v - 1) \times (360/V)$
- Amplitude: $A = 1.0$
- Frequency: $F = 300$ MHz ($\lambda = 1$)

Background:

- $\varepsilon_r = 1.0$
- $\sigma = 0$ [S/m]

Scatterer

- E-shaped object, $\ell_1 = \frac{5}{6}\lambda$, $\ell_2 = \lambda/2$
- $\varepsilon_r \in \{1.5,\ 2.0,\ 3.0\}$
- $\sigma = 0$ [S/m]

Born Iterative Method

- $I_{MAX} = 10$
- $\eta = 10^{-3}$

1.1.1 E-shaped Object, $\ell_1 = \frac{5}{6}\lambda$, $\ell_2 = \lambda/2$ - $\tau = 0.5$

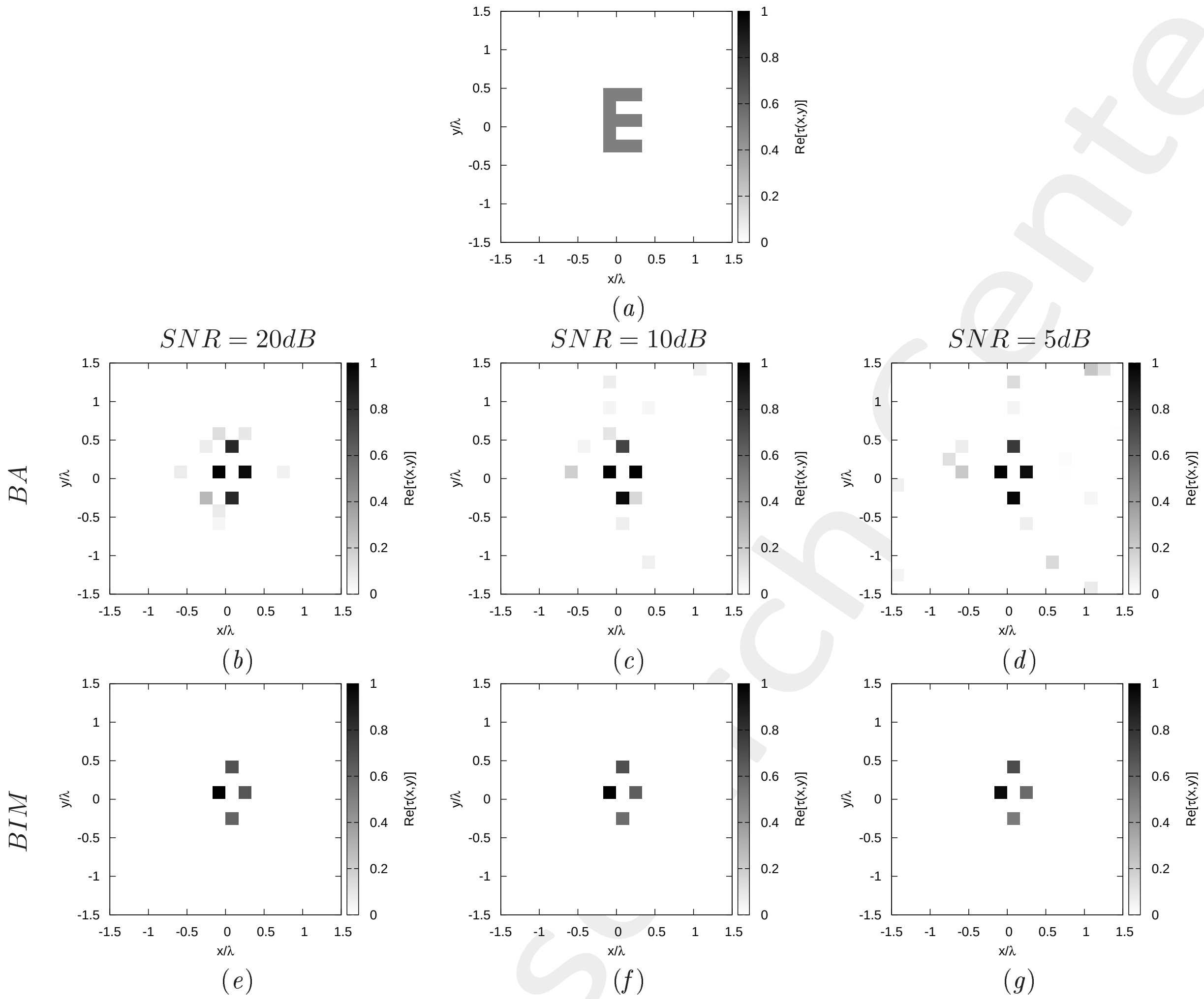

Figure 2: *E-shaped Object*, $\ell_1 = \frac{5}{6}\lambda$, $\ell_2 = \lambda/2$: (a) Direct problem with $\tau = 0.5$, (b) MT-BCS reconstructed profiles for $SNR = 20$ [dB], (c) $SNR = 10$ [dB] and (d) $SNR = 5$ [dB] with (b)-(d) First Born approximation, (e)-(g) Born Iterative Method

1.1.2 E-shaped Object, $\ell_1 = \frac{5}{6}\lambda$, $\ell_2 = \lambda/2$ - $\tau = 1.0$

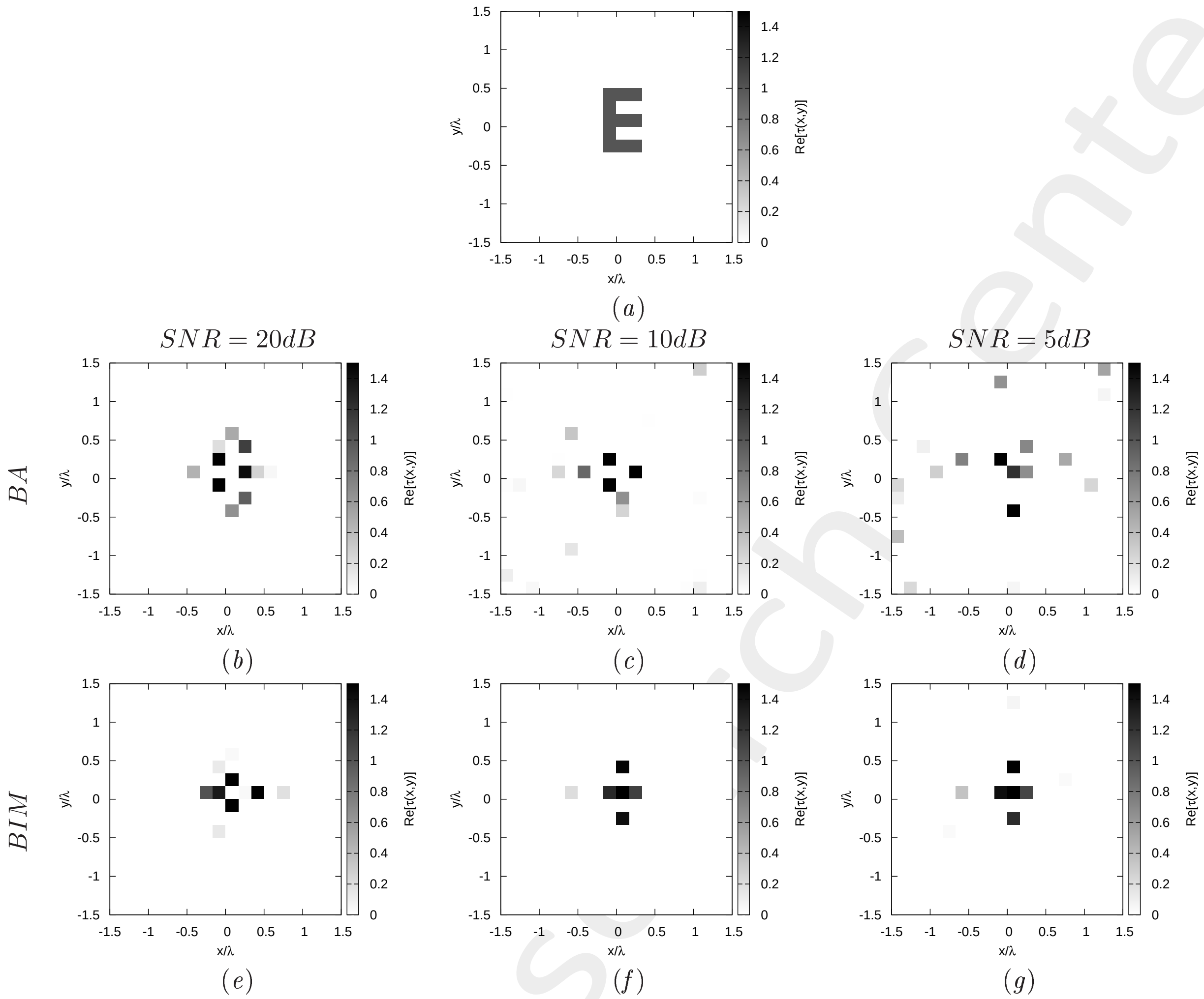

Figure 3: *E-shaped Object,* $\ell_1 = \frac{5}{6}\lambda$, $\ell_2 = \lambda/2$: (a) Direct problem with $\tau = 1.0$, $(b)(e)$ MT-BCS reconstructed profiles for $SNR = 20$ [dB], $(c)(f)$ $SNR = 10$ [dB] and $(d)(g)$ $SNR = 5$ [dB] with (b)-(d) First Born approximation, (e)-(g) Born Iterative Method

1.1.3 E-shaped Object, $\ell_1 = \frac{5}{6}\lambda$, $\ell_2 = \lambda/2$ - $\tau = 2.0$

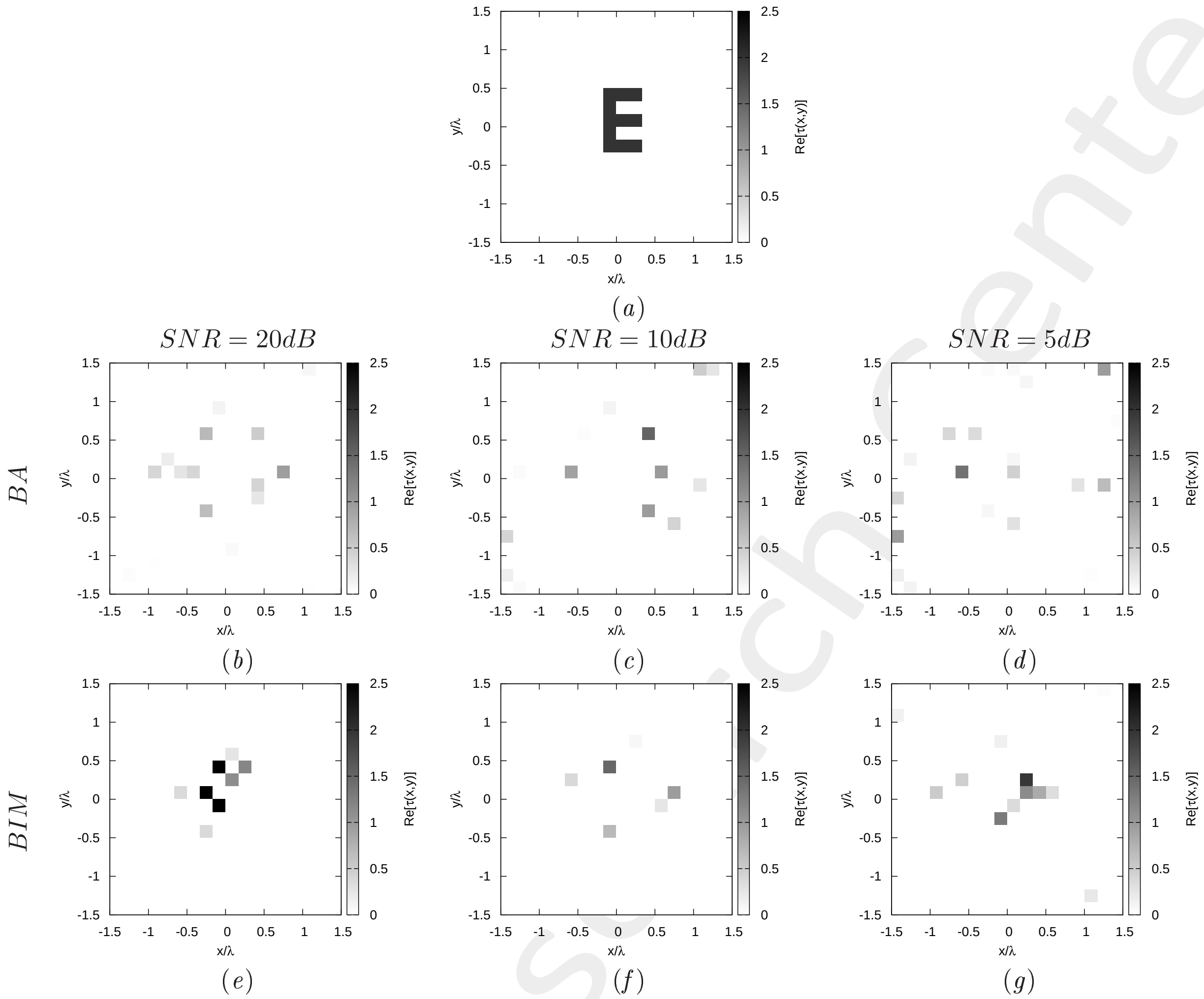

Figure 4: *E-shaped Object,* $\ell_1 = \frac{5}{6}\lambda$, $\ell_2 = \lambda/2$: (a) Direct problem with $\tau = 2.0$, $(b)(e)$ MT-BCS reconstructed profiles for $SNR = 20$ [dB], $(c)(f)$ $SNR = 10$ [dB] and $(d)(g)$ $SNR = 5$ [dB] with (b)-(d) First Born approximation, (e)-(g) Born Iterative Method

1.2 C-shaped Object, $\ell_1 = \frac{2}{3}\lambda$, $\ell_2 = \lambda/2$

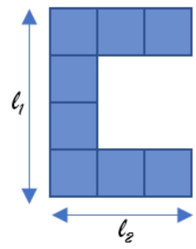

Figure 5: C-shaped Object

Test Case Description

Direct solver:

- Cubic domain divided in $\sqrt{D} \times \sqrt{D}$ cells
- Number of cells for the direct solver: $D = 1296$ (discretization $= \lambda/12$)

Inverse solver:

- Cubic domain divided in $\sqrt{N} \times \sqrt{N}$ cells
- Number of cells for the inversion: $N = 324$ (discretization $= \lambda/6$)

Measurement domain:

- Total number of measurements: $M = 27$
- Measurement points placed on circles of radius $\rho = 3\lambda$

Sources:

- Plane waves
- Number of views: $V = 4$; $\theta^v_{inc} = 0° + (v-1) \times (360/V)$
- Amplitude: $A = 1.0$
- Frequency: $F = 300$ MHz ($\lambda = 1$)

Background:

- $\varepsilon_r = 1.0$
- $\sigma = 0$ [S/m]

Scatterer

- C-shaped object, $\ell_1 = \frac{2}{3}\lambda$, $\ell_2 = \lambda/2$
- $\varepsilon_r \in \{1.5,\ 2.0,\ 3.0\}$
- $\sigma = 0$ [S/m]

Born Iterative Method

- $I_{MAX} = 10$
- $\eta = 10^{-3}$

1.2.1 C-shaped Object, $\ell_1 = \frac{2}{3}\lambda$, $\ell_2 = \lambda/2$ - $\tau = 0.5$

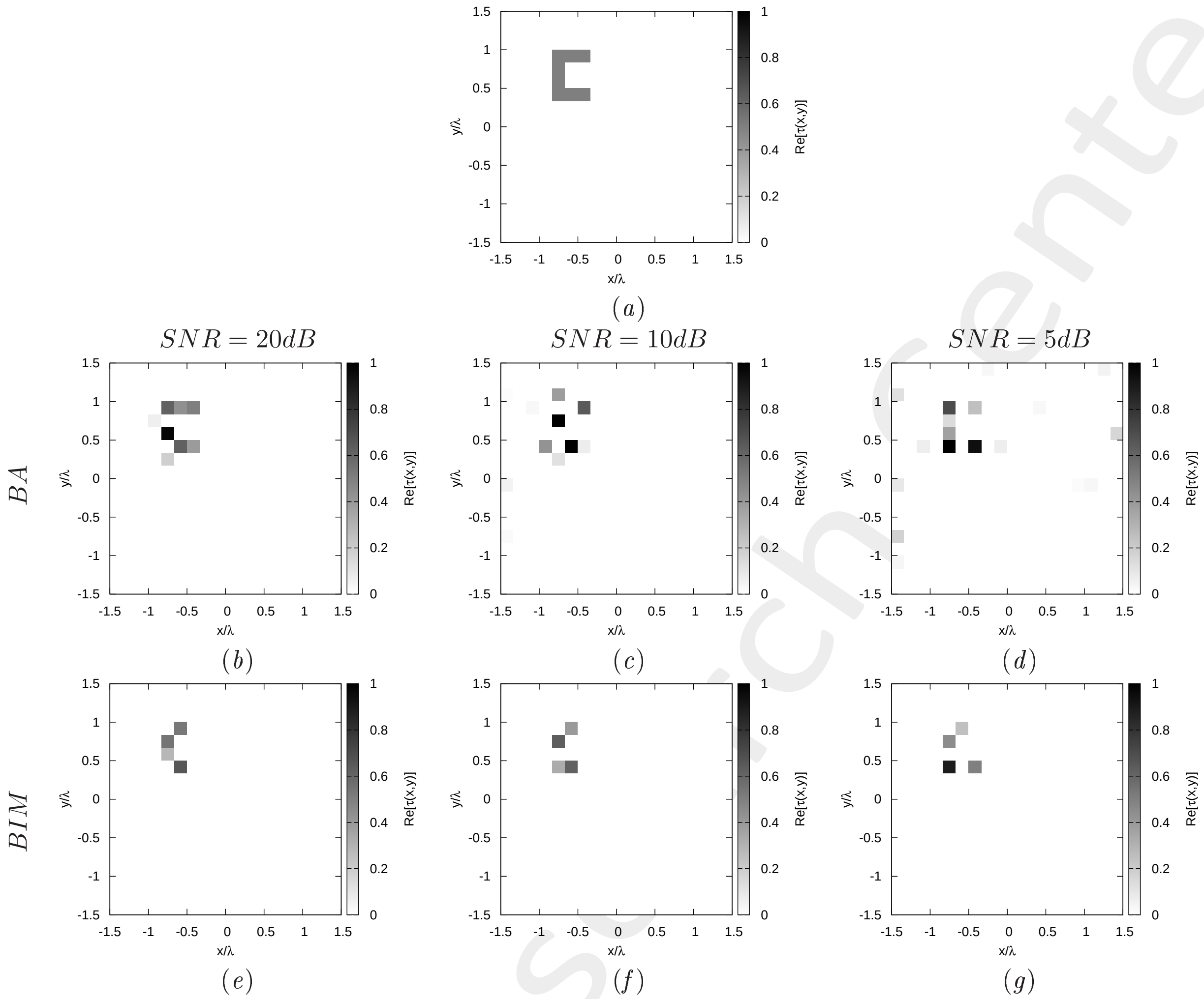

Figure 6: *C-shaped Object*, $\ell_1 = \frac{2}{3}\lambda$, $\ell_2 = \lambda/2$: (a) Direct problem with $\tau = 0.5$, (b) MT-BCS reconstructed profiles for $SNR = 20$ [dB], (c) $SNR = 10$ [dB] and (d) $SNR = 5$ [dB] with (b)-(d) First Born approximation, (e)-(g) Born Iterative Method

1.2.2 C-shaped Object, $\ell_1 = \frac{2}{3}\lambda$, $\ell_2 = \lambda/2$ - $\tau = 1.0$

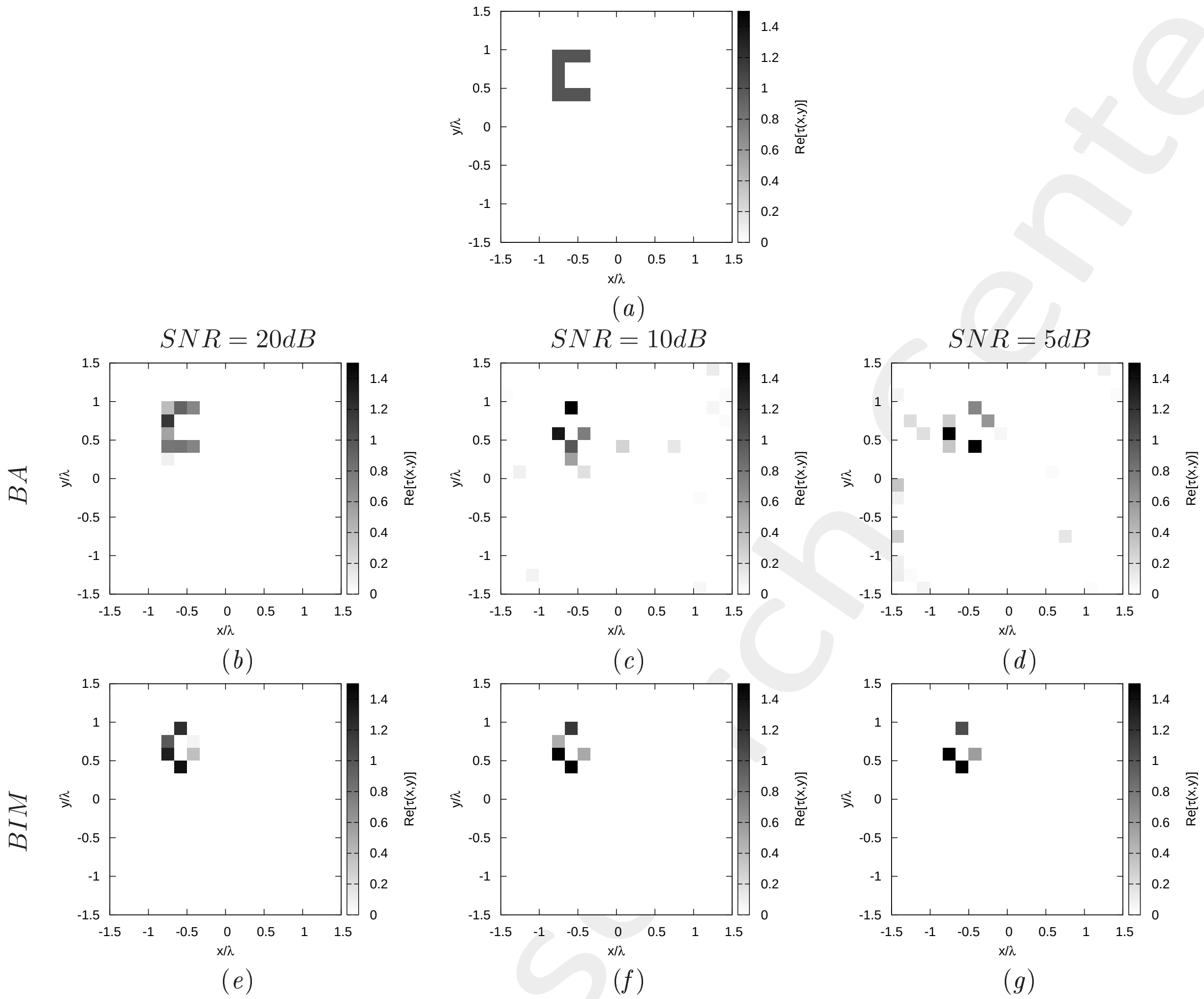

Figure 7: *C-shaped Object,* $\ell_1 = \frac{2}{3}\lambda$, $\ell_2 = \lambda/2$: (a) Direct problem with $\tau = 1.0$, $(b)(e)$ MT-BCS reconstructed profiles for $SNR = 20$ [dB], $(c)(f)$ $SNR = 10$ [dB] and $(d)(g)$ $SNR = 5$ [dB] with (b)-(d) First Born approximation, (e)-(g) Born Iterative Method

1.2.3 C-shaped Object, $\ell_1 = \frac{2}{3}\lambda$, $\ell_2 = \lambda/2$ - $\tau = 2.0$

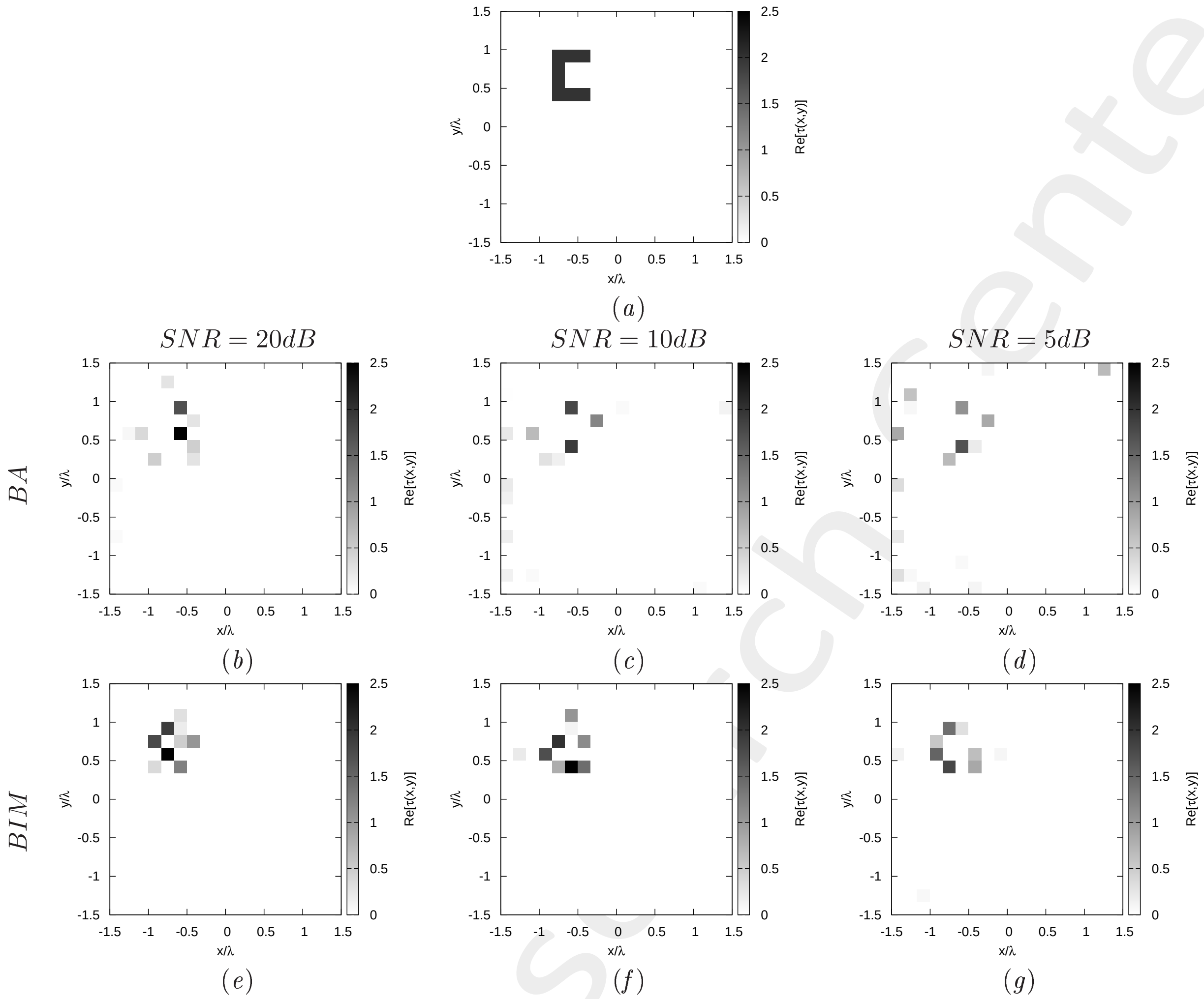

Figure 8: *C-shaped Object,* $\ell_1 = \frac{2}{3}\lambda$, $\ell_2 = \lambda/2$: (a) Direct problem with $\tau = 2.0$, $(b)(e)$ MT-BCS reconstructed profiles for $SNR = 20$ [dB], $(c)(f)$ $SNR = 10$ [dB] and $(d)(g)$ $SNR = 5$ [dB] with (b)-(d) First Born approximation, (e)-(g) Born Iterative Method

1.3 Rectangle-shaped Object, $\ell = \lambda/2$, $h = \lambda/3$

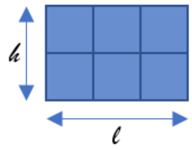

Figure 9: Rectangle-shaped Object

Test Case Description

Direct solver:

- Cubic domain divided in $\sqrt{D} \times \sqrt{D}$ cells
- Number of cells for the direct solver: $D = 1296$ (discretization $= \lambda/12$)

Inverse solver:

- Cubic domain divided in $\sqrt{N} \times \sqrt{N}$ cells
- Number of cells for the inversion: $N = 324$ (discretization $= \lambda/6$)

Measurement domain:

- Total number of measurements: $M = 27$
- Measurement points placed on circles of radius $\rho = 3\lambda$

Sources:

- Plane waves
- Number of views: $V = 4$; $\theta_{inc}^{v} = 0° + (v - 1) \times (360/V)$
- Amplitude: $A = 1.0$
- Frequency: $F = 300$ MHz ($\lambda = 1$)

Background:

- $\varepsilon_r = 1.0$
- $\sigma = 0$ [S/m]

Scatterer

- Rectangle-shaped object, $\ell = \lambda/2$, $h = \lambda/3$
- $\varepsilon_r \in \{1.5,\ 2.0,\ 3.0\}$
- $\sigma = 0$ [S/m]

Born Iterative Method

- $I_{MAX} = 10$
- $\eta = 10^{-3}$

1.3.1 Rectangle-shaped Object, $\ell = \lambda/2$, $h = \lambda/3$ - $\tau = 0.5$

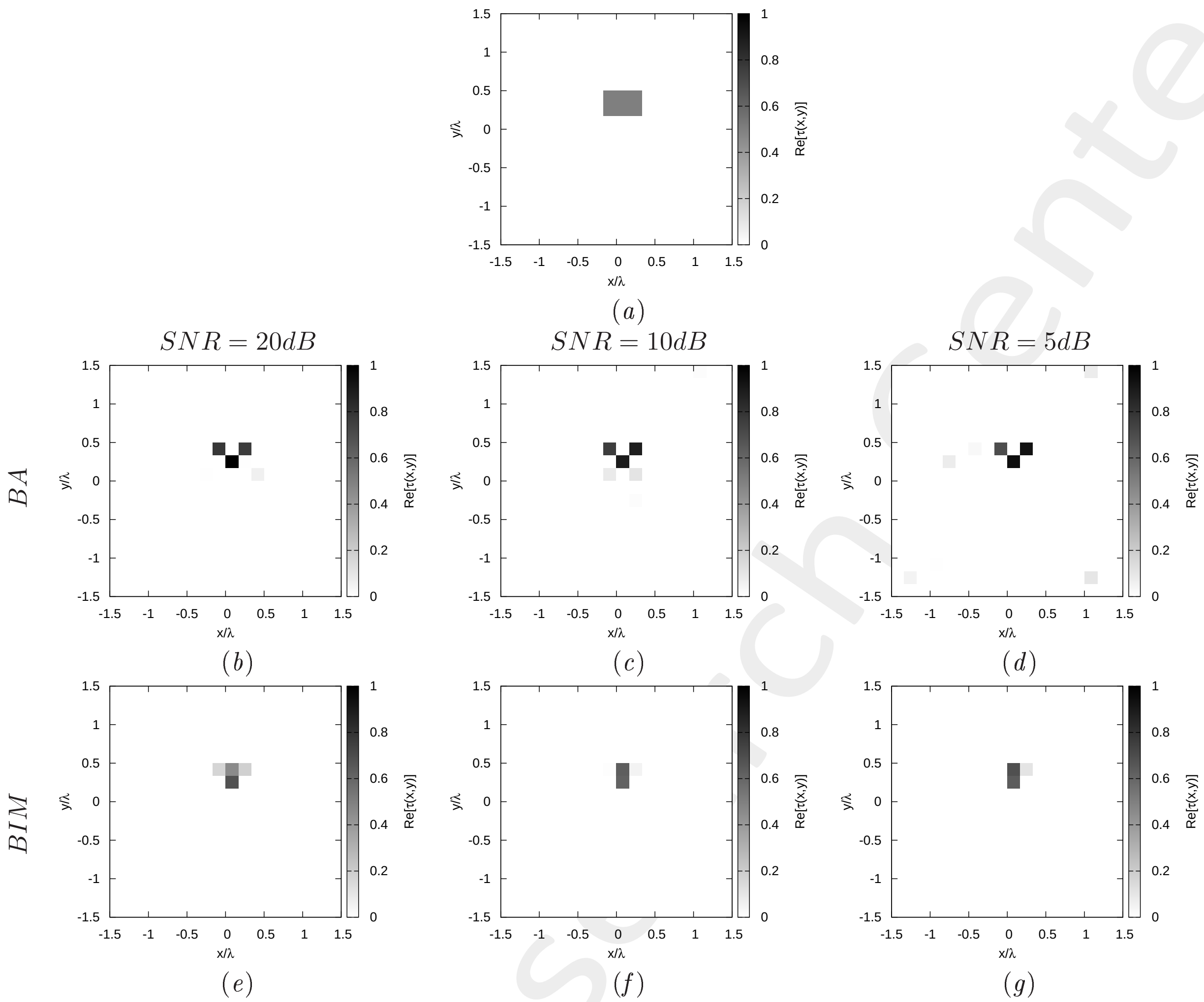

Figure 10: *Rectangle-shaped Object*, $\ell = \lambda/2$, $h = \lambda/3$: (a) Direct problem with $\tau = 0.5$, (b) MT-BCS reconstructed profiles for $SNR = 20$ [dB], (c) $SNR = 10$ [dB] and (d) $SNR = 5$ [dB] with (b)-(d) First Born approximation, (e)-(g) Born Iterative Method

1.3.2 Rectangle-shaped Object, $\ell = \lambda/2$, $h = \lambda/3$ - $\tau = 1.0$

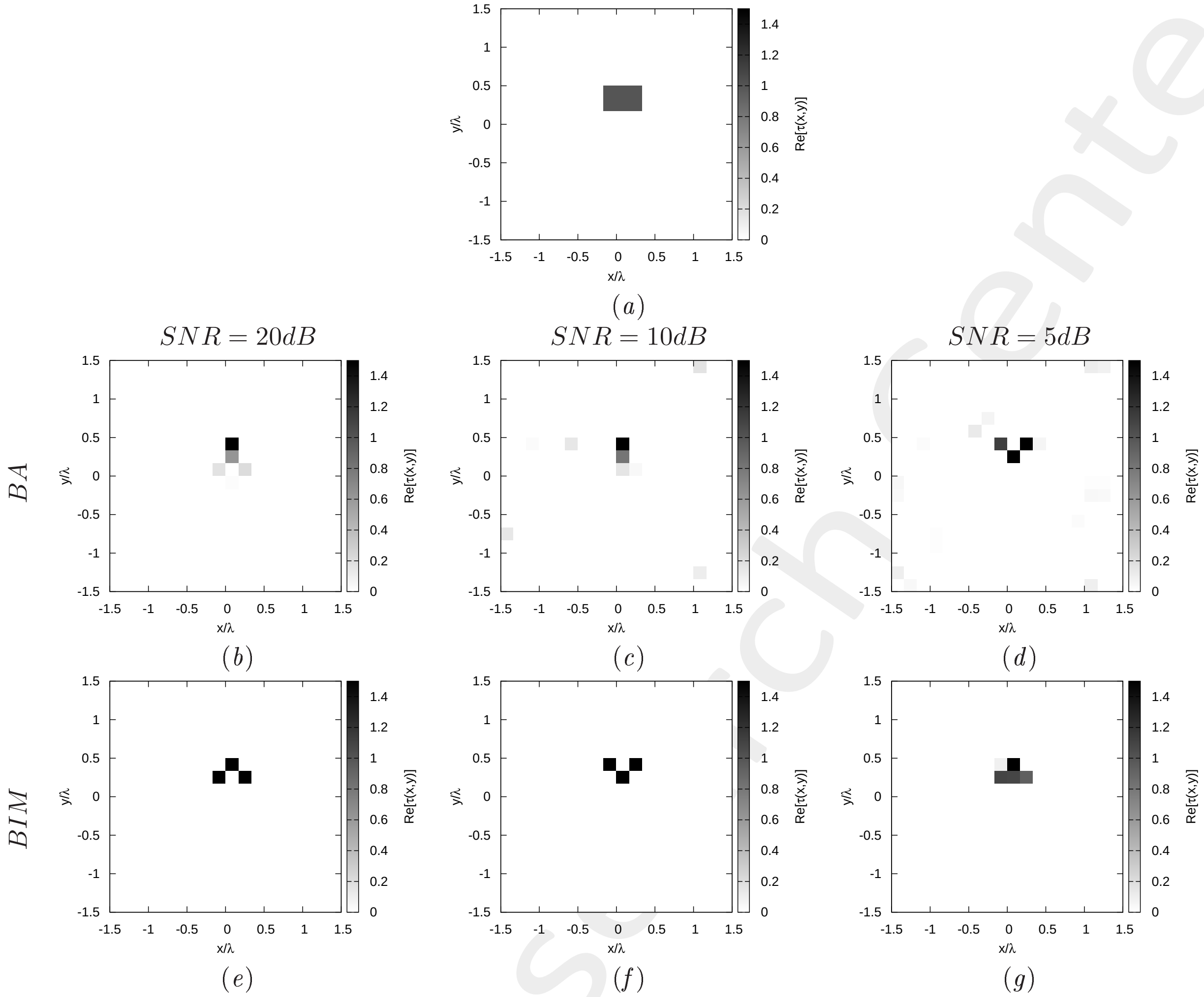

Figure 11: *Rectangle-shaped Object,* $\ell = \lambda/2$, $h = \lambda/3$: (a) Direct problem with $\tau = 1.0$, $(b)(e)$ MT-BCS reconstructed profiles for $SNR = 20$ [dB], $(c)(f)$ $SNR = 10$ [dB] and $(d)(g)$ $SNR = 5$ [dB] with (b)-(d) First Born approximation, (e)-(g) Born Iterative Method

1.3.3 Rectangle-shaped Object, $\ell = \lambda/2$, $h = \lambda/3$ - $\tau = 2.0$

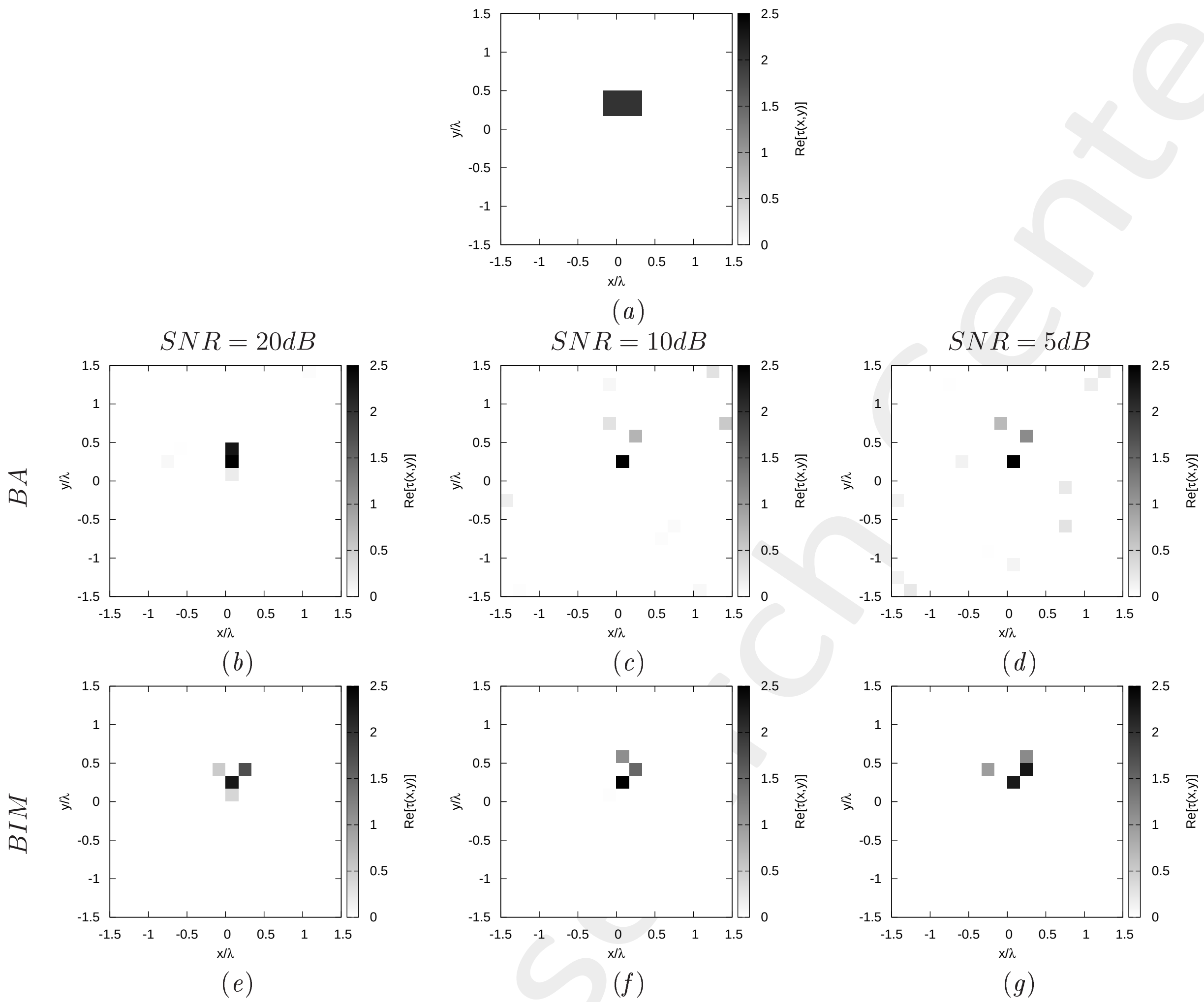

Figure 12: *Rectangle-shaped Object,* $\ell = \lambda/2$, $h = \lambda/3$: (a) Direct problem with $\tau = 2.0$, $(b)(e)$ MT-BCS reconstructed profiles for $SNR = 20$ [dB], $(c)(f)$ $SNR = 10$ [dB] and $(d)(g)$ $SNR = 5$ [dB] with (b)-(d) First Born approximation, (e)-(g) Born Iterative Method

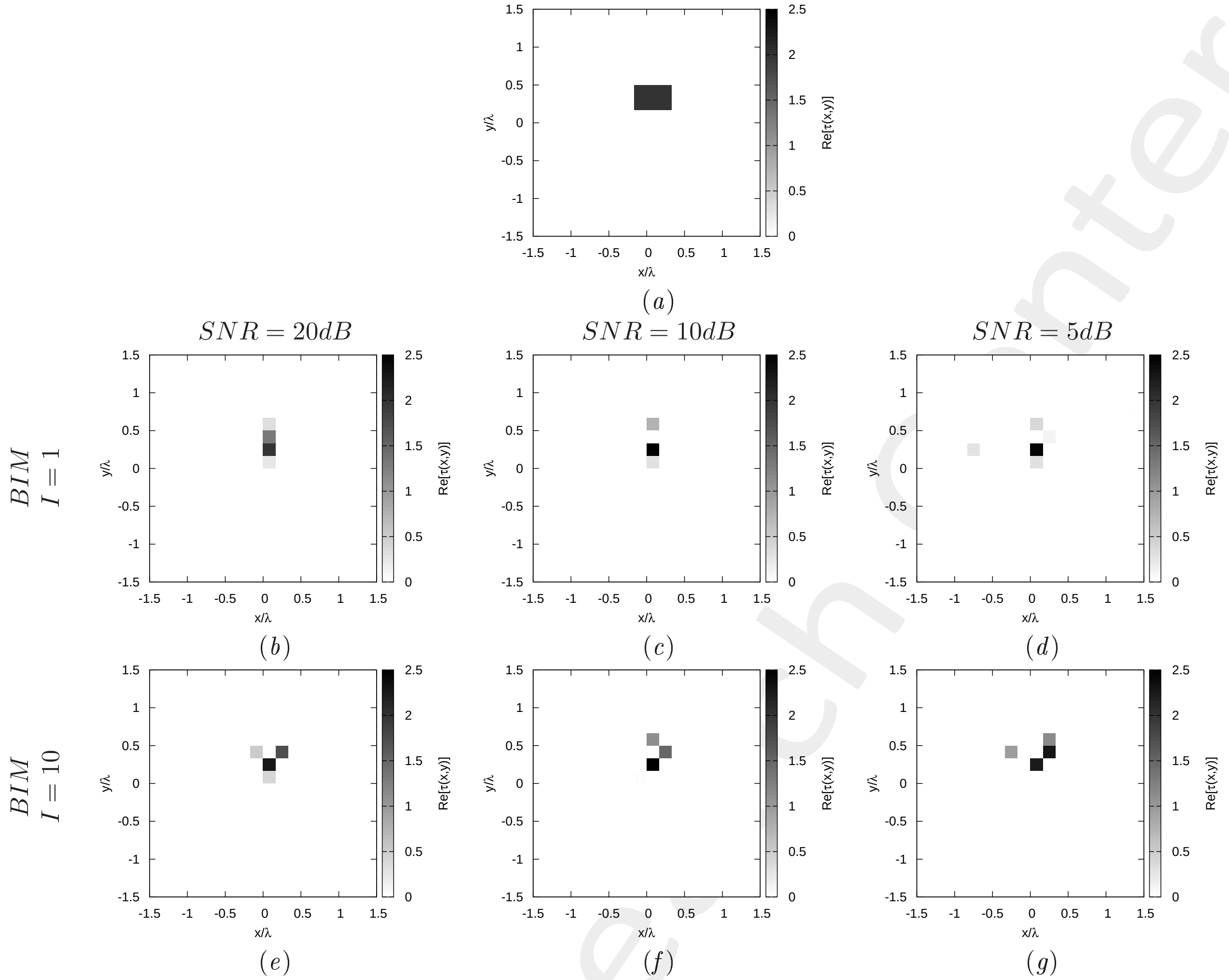

Figure 13: *Rectangle-shaped Object*, $\ell = \lambda/2$, $h = \lambda/3$: (a) Direct problem with $\tau = 2.0$, $(b)(e)$ MT-BCS reconstructed profiles for $SNR = 20$ [dB], $(c)(f)$ $SNR = 10$ [dB] and $(d)(g)$ $SNR = 5$ [dB] with (b)-(d) Born Iterative Method-$I = 1$, (e)-(g) Born Iterative Method- $I = 10$

1.4 Multiple Objects

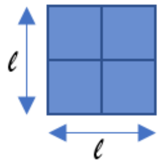

Figure 14: Square-shaped Object

Test Case Description

Direct solver:

- Cubic domain divided in $\sqrt{D} \times \sqrt{D}$ cells
- Number of cells for the direct solver: $D = 1296$ (discretization $= \lambda/12$)

Inverse solver:

- Cubic domain divided in $\sqrt{N} \times \sqrt{N}$ cells
- Number of cells for the inversion: $N = 324$ (discretization $= \lambda/6$)

Measurement domain:

- Total number of measurements: $M = 27$
- Measurement points placed on circles of radius $\rho = 3\lambda$

Sources:

- Plane waves
- Number of views: $V = 4$; $\theta_{inc}^{v} = 0° + (v - 1) \times (360/V)$
- Amplitude: $A = 1.0$
- Frequency: $F = 300$ MHz ($\lambda = 1$)

Background:

- $\varepsilon_r = 1.0$
- $\sigma = 0$ [S/m]

Scatterer

- 3 Square-shaped object, $\ell = \lambda/3$
- $\varepsilon_r \in \{1.5,\ 2.0,\ 3.0\}$
- $\sigma = 0$ [S/m]

Born Iterative Method

- $I_{MAX} = 10$
- $\eta = 10^{-3}$

1.4.1 Multiple Objects, $\tau = 0.5$

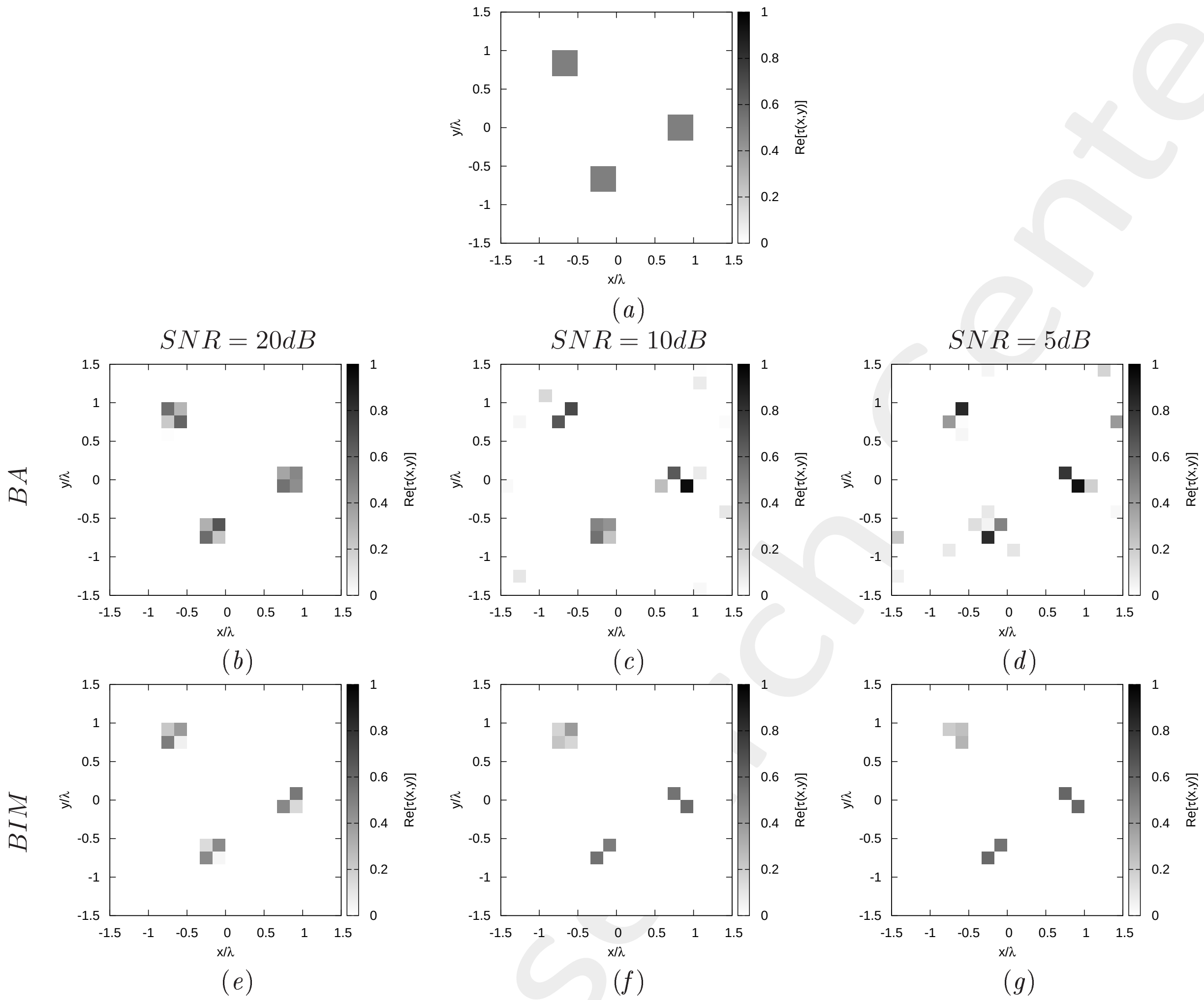

Figure 15: *Multiple Objects, 3 square-shaped Objects:*$\ell = \lambda/3$: (a) Direct problem with $\tau = 0.5$, (b) MT-BCS reconstructed profiles for $SNR = 20$ [dB], (c) $SNR = 10$ [dB] and (d) $SNR = 5$ [dB] with (b)-(d) First Born approximation, (e)-(g) Born Iterative Method

1.4.2 Multiple Object, $\tau = 1.0$

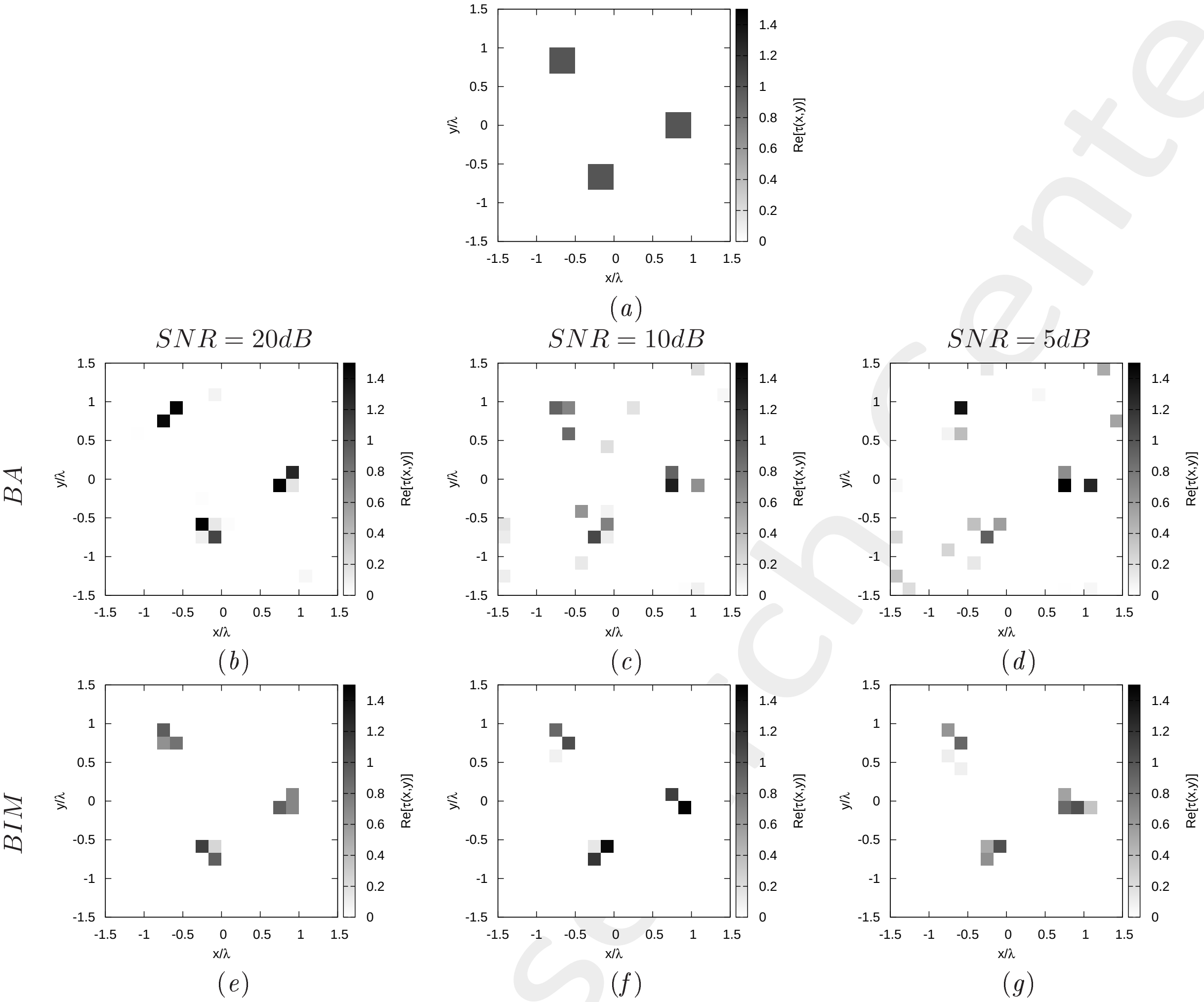

Figure 16: *Multiple Objects, 3 square-shaped Objects:*$\ell = \lambda/3$: (a) Direct problem with $\tau = 1.0$, $(b)(e)$ MT-BCS reconstructed profiles for $SNR = 20$ [dB], $(c)(f)$ $SNR = 10$ [dB] and $(d)(g)$ $SNR = 5$ [dB] with (b)-(d) First Born approximation, (e)-(g) Born Iterative Method

1.4.3 Multiple Objects, $\tau = 2.0$

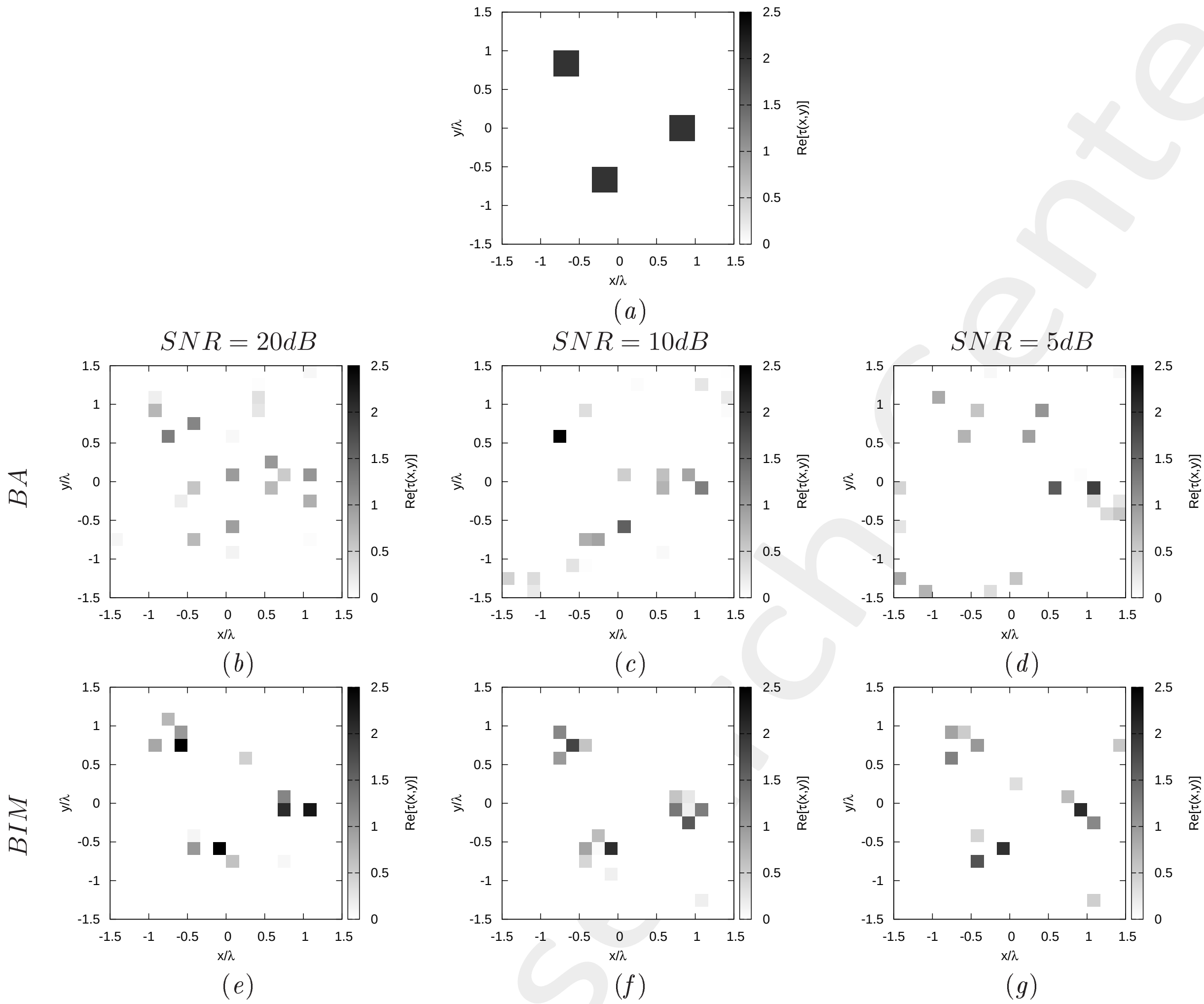

Figure 17: *Multiple Objects, 3 square-shaped Objects:*$\ell = \lambda/3$: (a) Direct problem with $\tau = 2.0$, $(b)(e)$ MT-BCS reconstructed profiles for $SNR = 20$ [dB], $(c)(f)$ $SNR = 10$ [dB] and $(d)(g)$ $SNR = 5$ [dB] with (b)-(d) First Born approximation, (e)-(g) Born Iterative Method

References

[1] G. Oliveri, M. Salucci, N. Anselmi, and A. Massa, "Compressive sensing as applied to inverse problems for imaging: theory, applications, current trends, and open challenges," *IEEE Antennas Propag. Mag.*, vol. 59, no. 5, pp. 34-46, Oct. 2017.

[2] A. Massa, P. Rocca, and G. Oliveri, "Compressive sensing in electromagnetics - A review," *IEEE Antennas Propag. Mag.*, pp. 224-238, vol. 57, no. 1, Feb. 2015.

[3] G. Oliveri, L. Poli, N. Anselmi, M. Salucci, and A. Massa, "Compressive sensing-based Born iterative method for tomographic imaging," *IEEE Trans. Microw. Theory Techn.*, vol. 67, no. 5, pp. 1753-1765, May 2019.

[4] M. Salucci, A. Gelmini, L. Poli, G. Oliveri, and A. Massa, "Progressive compressive sensing for exploiting frequency-diversity in GPR imaging," *Journal of Electromagnetic Waves and Applications*, vol. 32, no. 9, pp. 1164-1193, 2018.

[5] N. Anselmi, L. Poli, G. Oliveri, and A. Massa, "Iterative multi-resolution bayesian CS for microwave imaging," *IEEE Trans. Antennas Propag.*, vol. 66, no. 7, pp. 3665-3677, Jul. 2018.

[6] N. Anselmi, G. Oliveri, M. A. Hannan, M. Salucci, and A. Massa, "Color compressive sensing imaging of arbitrary-shaped scatterers," *IEEE Trans. Microw. Theory Techn.*, vol. 65, no. 6, pp. 1986-1999, Jun. 2017.

[7] N. Anselmi, G. Oliveri, M. Salucci, and A. Massa, "Wavelet-based compressive imaging of sparse targets," *IEEE Trans. Antennas Propag.*, vol. 63, no. 11, pp. 4889-4900, Nov. 2015.

[8] G. Oliveri, N. Anselmi, and A. Massa, "Compressive sensing imaging of non-sparse 2D scatterers by a total-variation approach within the Born approximation," *IEEE Trans. Antennas Propag.*, vol. 62, no. 10, pp. 5157-5170, Oct. 2014.

[9] L. Poli, G. Oliveri, and A. Massa, "Imaging sparse metallic cylinders through a local shape function Bayesian compressive sensing approach," *Journal of Optical Society of America A*, vol. 30, no. 6, pp. 1261-1272, 2013.

[10] L. Poli, G. Oliveri, F. Viani, and A. Massa, "MT-BCS-based microwave imaging approach through minimum-norm current expansion," *IEEE Trans. Antennas Propag.*, vol. 61, no. 9, pp. 4722-4732, Sep. 2013.

[11] L. Poli, G. Oliveri, P. Rocca, and A. Massa, "Bayesian compressive sensing approaches for the reconstruction of two-dimensional sparse scatterers under TE illumination," *IEEE Trans. Geosci. Remote Sens.*, vol. 51, no. 5, pp. 2920-2936, May 2013.

[12] L. Poli, G. Oliveri, and A. Massa, "Microwave imaging within the first-order Born approximation by means of the contrast-field Bayesian compressive sensing," *IEEE Trans. Antennas Propag.*, vol. 60, no. 6, pp. 2865-2879, Jun. 2012.

[13] G. Oliveri, L. Poli, P. Rocca, and A. Massa, "Bayesian compressive optical imaging within the Rytov approximation," *Optics Letters*, vol. 37, no. 10, pp. 1760-1762, 2012.

[14] G. Oliveri, P. Rocca, and A. Massa, "A Bayesian compressive sampling-based inversion for imaging sparse scatterers," *IEEE Trans. Geosci. Remote Sens.*, vol. 49, no. 10, pp. 3993-4006, Oct. 2011.

[15] M. Salucci, A. Gelmini, G. Oliveri, and A. Massa, "Planar arrays diagnosis by means of an advanced Bayesian compressive processing," *IEEE Trans. Antennas Propag.*, vol. 66, no. 11, pp. 5892-5906, Nov. 2018.

[16] L. Poli, G. Oliveri, P. Rocca, M. Salucci, and A. Massa, "Long-distance WPT unconventional arrays synthesis," *Journal of Electromagnetic Waves and Applications*, vol. 31, no. 14, pp. 1399-1420, Jul. 2017.

[17] G. Oliveri, M. Salucci, and A. Massa, "Synthesis of modular contiguously clustered linear arrays through a sparseness-regularized solver," *IEEE Trans. Antennas Propag.*, vol. 64, no. 10, pp. 4277-4287, Oct. 2016.

[18] P. Rocca, M. A. Hannan, M. Salucci, and A. Massa, "Single-snapshot DoA estimation in array antennas with mutual coupling through a multi-scaling BCS strategy," *IEEE Trans. Antennas Propag.*, vol. 65, no. 6, pp. 3203-3213, Jun. 2017.

[19] M. Salucci, L. Poli, and G. Oliveri, "Full-vectorial 3D microwave imaging of sparse scatterers through a multi-task Bayesian compressive sensing approach," *Journal of Imaging*, vol. 5, no. 1, pp. 1-24, Jan. 2019 (DOI: 10.3390/jimaging5010019).